PHYSICAL REVIEW E VOLUME 56, NUMBER 6 DECEMBER 1997

Oscillatory instabilities in rapid directional solidification

M. Conti
Dipartimento di Matematica e Fisica, Università di Camerino, 62032 Camerino, Italy
(Received 28 July 1997)

The rapid directional solidification of a binary alloy is studied with the phase-field model. An oscillatory instability is evidenced which originates alternating low and high concentration solute bands. This instability, which is related to the banded structure observed in rapid solidification experiments, is predicted by previous studies conducted within the free-boundary formulation of the problem, incorporating nonequilibrium effects as solute trapping. In the present paper the governing equations of the model are numerically solved to show under what conditions (i.e., isotherm velocity and temperature gradient) the banded structure can be observed. [S1063-651X(97)51211-6]

PACS number(s): 81.10.Aj, 05.70.Ln, 64.70.Dv

In rapidly solidified alloys a structure has been observed consisting of a regular succession of dark and light bands, parallel to the solid-liquid front, with a band spacing ranging from 0.3 to 1.5 μm [1]. The dark bands have a precipitate structure, either cellular-dendritic or eutectic, depending on the alloy composition; the light bands show a uniform solute concentration. In order to explain the occurrence of this so-called *banded structure*, which is not expected within the classic Mullins-Sekerka stability analysis, the growth process has been addressed modifying the free-boundary diffusional model to incorporate nonequilibrium effects as solute trapping [2,3]; along these lines an oscillatory instability has been detected which is characterized by an infinite wavelength along the solid-liquid front. Karma and Sarkissian [4,5] extended this analysis, accounting for the diffusion of the latent heat released at the interface; the most relevant consequence of this effect is the reduction of the parameter range where the banded structure should occur. In a numerical study these authors [5] showed that the oscillatory instability actually leads, in a nonlinear regime, to periodic variations of the solute concentration along the growth direction (referred in the following as *solute bands*). While their analysis, conducted in one dimension, suppresses transverse morphological instabilities, it has been argued that it still captures the essential part of the banding phenomenon.

To better understand the mechanism underlying the formation of the banded structure, a different way not yet attempted could be based on the phase-field model (PFM). This approach, initially applied to the solidification of pure substances, was extended to describe alloy solidification [6–8]. Within this method a phase field $\phi(x,t)$ characterizes the phase of the system at each point; a free-energy (or entropy) functional is then constructed, depending on ϕ as well as on the local temperature and solute concentration T, c; a gradient term accounts for the energy cost associated with the solid-liquid interface. The extremization of the functional in respect to these variables results in the dynamic equations for the process. In the present study the rapid solidification of a binary alloy, driven by a moving temperature field, is simulated in one dimension through the phase-field model. Due to numerical tractability, the effect of the latent heat diffusion is neglected; it will be shown that an oscillatory instability which arises in a region of the parameters space, originates solute bands.

The system is an ideal binary solution with constituents A (solvent) and B (solute). Initially a solid ($x<x_0$) and a liquid ($x>x_0$) region are separated by an interface at temperature T_I. The solute concentration in the solid and liquid phases is fixed to the equilibrium values at T_I. Then the temperature field, characterized by a positive uniform gradient G, is pulled towards the positive x direction at constant velocity V_0, and the solidification front follows the advancing isotherms. This arrangement is well representative of standard directional solidification experiments, when heat diffusion is much faster than solute diffusion, and allows to decouple the temperature from the concentration and the phase fields. The problem will be treated scaling lengths to some reference length ξ and time to ξ^2/D_l, D_l being the solute diffusivity in the liquid phase. The model is presented in full detail in [9]; in the limit $(T-T_I)\ll T_I$ the governing equations become

$$\frac{\partial\phi}{\partial t}=[(1-c)m^A+cm^B]\times[\nabla^2\phi+(1-c)Q^A(T,\phi)+cQ^B(T,\phi)], \tag{1}$$

$$\frac{\partial c}{\partial t}=\nabla\cdot\{\lambda(\phi)\nabla c-c(1-c)\lambda(\phi)[H^A(\phi,T)-H^B(\phi,T)]\times\nabla\phi-c(1-c)\lambda(\phi)\Gamma(\phi,T)\nabla T\}, \tag{2}$$

$$\frac{\partial T}{\partial t}=-V_0\frac{\partial T}{\partial x}=-V_0G, \tag{3}$$

where

$$H^{A,B}(\phi,T)=W^{A,B}\frac{dg(\phi)}{d\phi}-L^{A,B}\frac{v_m}{R}\frac{dp(\phi)}{d\phi}\frac{T-T^{A,B}}{TT^{A,B}}, \tag{4}$$

$$Q^{A,B}=-\frac{\xi^2}{(h^{A,B})^2}\frac{dg(\phi)}{d\phi}-+\frac{1}{6\sqrt{2}}\frac{\xi^2L^{A,B}}{\sigma^{A,B}h^{A,B}}\frac{T-T^{A,B}}{T_I}\frac{dp(\phi)}{d\phi}, \tag{5}$$

$$\Gamma(\phi,T)=\frac{p(\phi)}{T^2}\frac{v_m}{R}(L^B-L^A), \tag{6}$$

$$\lambda(\phi)=\frac{D_s}{D_l}+p(\phi)\left(1-\frac{D_s}{D_l}\right). \quad (7)$$

In the above equations $g(\phi)=\frac{1}{4}\phi^2(1-\phi)^2$ is a symmetric double well potential with equal minima at $\phi=0$ and $\phi=1$; $p(\phi)$ is a monotonically increasing function of ϕ from $p(0)=0$ in the solid to $p(1)=1$ in the liquid; with the choice $p(\phi)=\phi^3(10-15\phi+6\phi^2)$ the bulk solid and liquid are described by $\phi=0$ and $\phi=1$, respectively, for every value of temperature. The function $\lambda(\phi)$ describes the smooth transition of the bulk solute diffusivity from D_s (in the solid) to D_l (in the liquid); v_m is the molar volume and R is the gas constant; $L^{A,B}$, $T^{A,B}$, and $\sigma^{A,B}$ indicate latent heat, melting temperature, and surface tension of pure components A and B, respectively; $h^{A,B}$ is the interface thickness of pure A (or B). The model parameters $m^{A,B}$, $W^{A,B}$ were associated with the physical properties of the alloy components by Warren and Boettinger [9],

$$m^{A,B}=\frac{\beta^{A,B}\sigma^{A,B}T^{A,B}}{D_l L^{A,B}}, \quad W^{A,B}=\frac{12}{\sqrt{2}}\frac{v_m}{R}\frac{\sigma^{A,B}}{T^{A,B}h^{A,B}}, \quad (8)$$

where $\beta^{A,B}$ is the kinetic undercooling coefficient of pure A or B, which relates the interface undercooling to the interface velocity v through $v=\beta^{A,B}(T^{A,B}-T)$. To estimate the above parameters we referred to the thermophysical properties of nickel (solvent) and copper (solute); the solute diffusivity in the solid phase was estimated as $D_s=10^{-6}D_l$. The length scale was fixed at $\xi=2.1\times10^{-4}$ cm and a realistic value for the interface thickness was selected of 1.68×10^{-7} cm. With this choice the results are $W^A=0.965$; $W^B=0.961$; $m^A=353.5$; $m^B=350$.

The evolution of Eqs. (1)–(3) has been considered in one spatial dimension, in the domain $0\leqslant x\leqslant x_m$ with x_m large enough to prevent finite-size effects. To verify the consistency of the numerical scheme at each time step solute conservation was checked, and verified within 0.001%. Except for temperatures, dimensionless units will be used to illustrate the numerical results. The initial concentration of the alloy is set to $c_{-\infty}=0.056\,09$ for the solid phase ($x<x_0$; $\phi=0$) and $c_{+\infty}=0.070\,68$ for the liquid phase ($x>x_0$; $\phi=1$). This corresponds to an equilibrium temperature $T_I=1706.06$ K. Then the initial temperature profile, defined as $T(x,0)=T_I+G(x-x_0)$ is pulled towards the positive x direction with constant velocity V_0.

Plots of the interface velocity versus time are shown in Figures 1(a) and 1(b) for $V_0=1200$ and $V_0=700$, respectively; the temperature gradient is $G=40$ K. When $V_0=1200$ the effect of initial conditions is rapidly lost; the front velocity v (and the interface temperature T_I) undergoes few damped oscillations before reaching the final steady state with $v=V_0$. On the contrary, at $V_0=700$ the process never reaches a steady regime, and the interface velocity continuously oscillates around the average value V_0. The oscillatory instability observed in Fig. 1(b) traces its roots to the nonmonotonic dependence $T_I(v)$ of the interface temperature on the interface velocity: due to suppression of solute partitioning (and to the reduction of solute concentration on the liquid side of the interface) at low velocity $T_I(v)$ first rises, then falls with increasing v reflecting the increasing undercooling required to advance the solidifying front. In the range with positive slope the driving force for the process (i.e., the dynamic undercooling) is a decreasing function of the associated flux (the growth rate) and instabilities must be expected. Aziz and Boettinger [10] determined the $T_I(v)$ dependence for steady growth within the continuous growth model, as

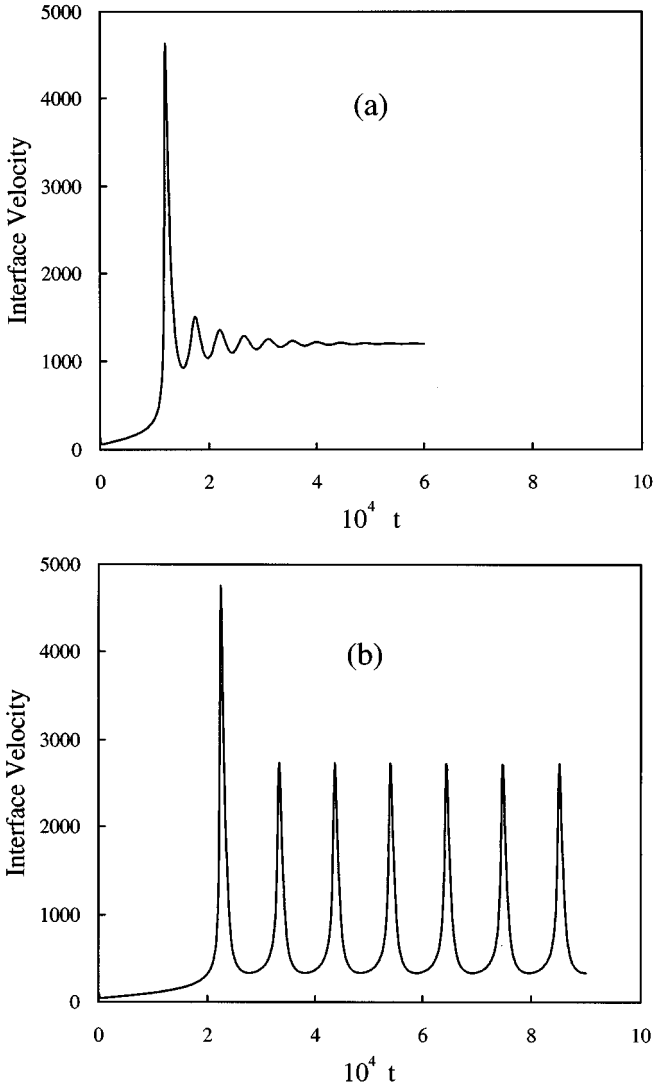

FIG. 1. (a) Interface velocity vs time. The isotherm velocity is $V_0=1200$ and the temperature gradient is $G=40$ K. (b) Interface velocity vs time. The isotherm velocity is $V_0=700$ and the temperature gradient is $G=40$ K.

$$T_I=T^A+\frac{m_l c_{+\infty}}{k}\frac{[1-k+\gamma\ln(k/k_e)]}{1-k_e}-\frac{v}{\beta^A}, \quad (9)$$

where m_l is the slope of the equilibrium liquidus line and k_e, k are the equilibrium and the velocity dependent partition coefficients, respectively; the parameter γ is equal to k or equal to unity depending on whether or not solute drag [10] is neglected in the dissipation of the free-energy that drives solidification. It is known [7] that Eq. (9) with $\gamma=1$ well represents the $T_I(v)$ dependence originated by the phase-field model. Figure 2 shows $T_I(v)$ as given by Eq. (9) with $\gamma=1$ (solid curve); the vertical line indicates the isotherm

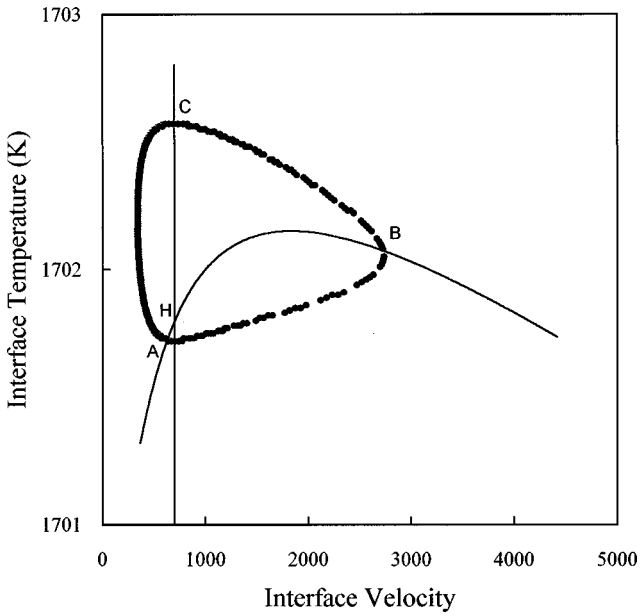

FIG. 2. Orbit followed by the process in the (T_I, v) plane; the isotherm velocity is indicated by the vertical line ($V_0 = 700$); $G = 40$ K. The meaning of the points A, B, C, H is illustrated in the text.

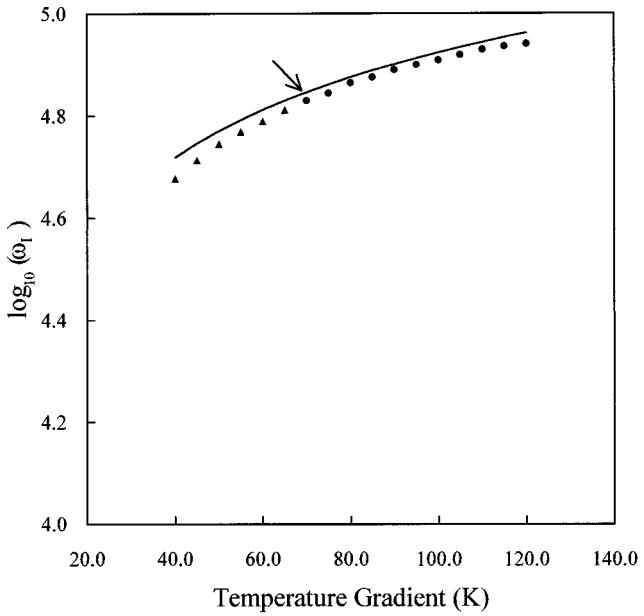

FIG. 4. Oscillation frequency vs the temperature gradient; the isotherm velocity is $V_0 = 600$. Solid line: as predicted by the linear stability analysis; the arrow marks the upper limit of the instability range. Solid circles and solid triangles: damped and undamped oscillatory solutions found in the present simulations.

velocity $V_0 = 700$. This value fixes the operating point for the process on the unstable branch of the curve (point H), and steady state solidification is not allowed. The solids dots represent the actual orbit followed by the process in the T_I, v plane with $V_0 = 700$: for the most part of the cycle the interface velocity is slightly lower than V_0, and the interface cools down; then the orbit traverses the $T_I(v)$ curve at point A and with a strong acceleration reaches point B on the stable branch. Here the interface velocity is much higher than V_0, and the interface warms up: solidification is strongly decelerated and the operating point shifts to C. Notice that the shape of the cycle can be modified when the latent heat diffusion is taken into account [5].

Merchant and Davis [3] performed a linear stability analysis of the free-boundary diffusional equations, neglecting the latent heat effect and imposing interface conditions along the results of the continuous growth model; assuming a periodic perturbation parallel to the advancing front of the form $\exp(iqy+\omega t)$ they determined the region in the parameters

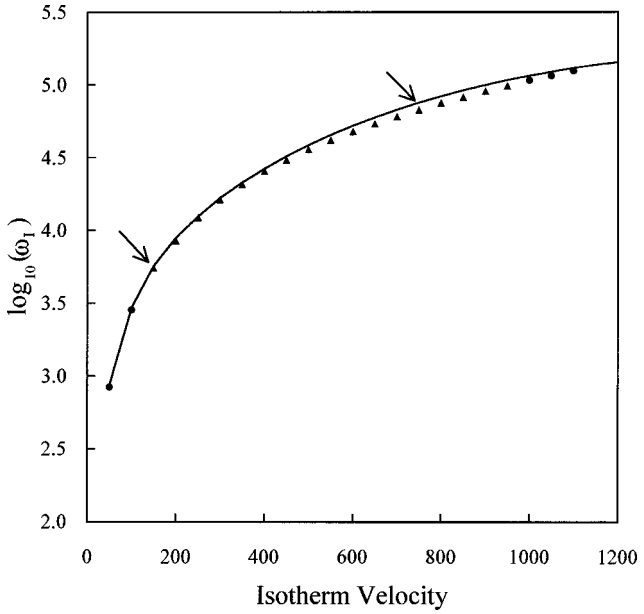

FIG. 3. Oscillation frequency vs the isotherm velocity; $G = 40$ K. Solid line: as predicted by the linear stability analysis. Solid circles and solid triangles: damped and undamped oscillatory solutions found in the present simulations. Within the arrows the linear stability analysis gives $\mathrm{Re}(\omega) > 0$.

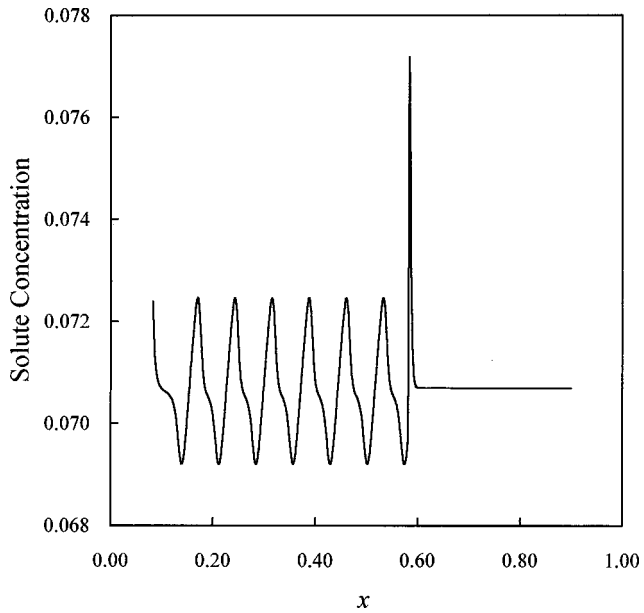

FIG. 5. Solute concentration profile along the growth direction. The isotherm velocity is $V_0 = 700$, and the temperature gradient is $G = 40$ K.

space where the oscillatory instability should arise, i.e., where $\mathrm{Re}(\omega)>0$ and $\omega_I=\mathrm{Im}(\omega)\neq 0$; the dependence of the oscillation frequency on the relevant parameters that characterize the process was also determined. Their results are compared to our present simulations in Fig. 3, where the oscillation frequency is represented versus the isotherm velocity, with $G=40$ K. The solid line corresponds to the predictions of the linear analysis; within the arrows $\mathrm{Re}(\omega)>0$, and undamped oscillations must be expected. The solid dots and solid triangles give the results of our simulations and correspond to damped and undamped oscillatory solutions, respectively. The range of unstable solutions determined with the phase-field model is slightly more extended than the one predicted by the free-boundary model; however, it can be observed that the agreement between the two sets of results is quite satisfactory. Figure 4 shows ω_I versus the temperature gradient G, with $V_0=600$: here, too, the results obtained with the phase-field model closely agree with the predictions of the free-boundary model; in both cases due to the stabilizing effect of the temperature gradient the oscillatory behavior is suppressed for $G>70$ K. The structure of the solidified alloy is strongly influenced by the interface dynamics. When $\mathrm{Re}(\omega)<0$ and $\omega_I=\mathrm{Im}(\omega)\neq 0$ the concentration profile in the solid phase shows few oscillations along a distance corresponding to the initial transient; when the steady regime is reached the composition of the solidified alloy corresponds to the liquid composition at infinity. A quite different situation can be observed in Fig. 5, where $V_0=700$ and $G=40$, corresponding to $\mathrm{Re}(\omega)>0$ (see Fig. 3). In this case the steady regime is never reached, and the periodic structure in the solid phase reflects the periodic variations of the interface velocity and temperature. The wavelength of the solute concentration profile has been estimated as $\lambda=0.0724$, which is practically coincident with the expected value $2\pi V_0/\omega_I=0.0727$.

In summary, the phase-field model has been proven to be able to predict the oscillatory regime that characterizes the interface dynamics in a region of the parameters space; the dependence of the oscillation frequency on both the temperature gradient and the interface velocity is in quite close agreement with the results of a linear stability analysis conducted in a sharp interface context. Due to numerical tractability, in the present study we neglected the latent heat released at the solid-liquid interface, assuming an infinite thermal diffusivity. As shown by Karma and Sarkissian [5] relaxing this approximation leads to an increase of the effective temperature gradient probed by the advancing front, and to a reduction of the parameters range where the oscillatory instability should be expected; nonetheless, the basic mechanism underlying the formation of solute bands should have been properly evidenced. In view of future extensions and refinements in this subject, it is worth noting that the phase-field model allows an easy description of rapid solidification processes even for concentrated solutions, with no limitations due to the actual shape of the alloy phase diagram, while at present the free-boundary approach can only be applied to very dilute solutions, when the alloy phase diagram can be conveniently linearized.

[1] For a review, see W. Kurz and R. Trivedi, Acta Metall. **38**, 1 (1990).
[2] S. R. Coriell and R. F. Sekerka, J. Cryst. Growth **61**, 499 (1983).
[3] G. J. Merchant and S. H. Davis, Acta Metall. Mater. **38**, 2683 (1990).
[4] A. Karma and A. Sarkissian, Phys. Rev. Lett. **27**, 2616 (1992).
[5] A. Karma and A. Sarkissian, Phys. Rev. E **47**, 513 (1993).
[6] A. A. Wheeler, W. J. Boettinger, and G. B. McFadden, Phys. Rev. A **45**, 7424 (1992).
[7] A. A. Wheeler, W. J. Boettinger, and G. B. McFadden, Phys. Rev. E **47**, 1893 (1993).
[8] G. Caginalp and J. Jones, Ann. Phys. (N.Y.) **237**, 66 (1995).
[9] J. A. Warren and W. J. Boettinger, Acta Metall. Mater. **43**, 689 (1995).
[10] M. J. Aziz and W. J. Boettinger, Acta Metall. **42**, 527 (1994).